MATEMATIKA, MJIAM, Volume 42, Number 1, 49–71

Modeling of Double-Lane Roundabouts Using the Waiting System

[1]Cheah Yuat Hoong[*] and [2]Yeak Su Hoe

[1]Xiamen University Malaysia,
Jalan Sunsuria, Bandar Sunsuria, 43900 Sepang, Selangor, Malaysia.

[2]Department of Mathematical Sciences, Universiti Teknologi Malaysia,
81310 UTM Johor Bahru, Johor, Malaysia.

[*]Corresponding author: y_hoong0617@yahoo.com

Article history
Received: 10 February 2025
Received in revised form: 17 September 2025
Accepted: 29 October 2025
Published on line: 30 April 2026

Abstract Roundabouts are designed to improve intersection safety and efficiency, and in Malaysia, most are double-laned. However, existing methods for analysing roundabout performance remain limited. Some focus only on traffic parameters or signal controls without considering density and flux variations, while others treat double-lane roundabouts as separate, independent lanes or restrict analysis to entry and exit points. These approaches do not fully capture the dynamics of a complete double-lane four-arm roundabout. To address this gap, a new double-lane roundabout model is derived. The model represents the roundabout as two interconnected rings with four arms and incorporates a waiting system to better reflect real traffic conditions. It is formulated using hyperbolic partial differential equations within a macroscopic framework and solved numerically with the Godunov method. The Courant-Friedrichs-Lewy (CFL) condition is applied to ensure stability and accuracy of the simulations. Simulation results demonstrate logical changes in Total Travel Time and Total Waiting Time under different parameter settings, reflecting realistic traffic flow behaviour. This model provides a more comprehensive representation of double-lane roundabouts, offering valuable insights for researchers as well as government and private agencies in evaluating roundabout performance.

Keywords Double-lane roundabouts; Waiting system; CFL condition; Macroscopic model.

Mathematics Subject Classification 35L02, 35L65.

1 Introduction

Roundabouts are a very popular design solution for intersecting roads and have been used widely in both urban and rural areas as they are highly safe, can prevent delays, and can reduce pollutant emissions from moving vehicles [1]. A roundabout is a circular intersection design where the entering traffic must yield to circulating traffic at low speed around a central island. The geometry of a roundabout controls how fast traffic enters and moves through

the intersection. This design reduces the severity of collisions, encourages drivers to yield to pedestrians, and gives drivers more time to judge and enter a safe gap in traffic [2]. Another important role of a roundabout is in the handling of high traffic volumes [3] whereby it helps ease the traffic flow.

Numerous surveys worldwide have indicated that the second lane along the circulatory roadway contributes to a 30% increase in capacity [4] and that the safety benefits are generally greater for single-lane roundabouts than double-lane roundabouts. However, in cases where single-lane roundabouts could not satisfy traffic or geometric conditions, it is necessary to adopt a double-lane roundabout [5]. The 2019 Insurance Institute for Highway Safety (IIHS) study indicates that the safety of double-lane roundabouts has improved over time, as drivers become more familiar with them [6]. The study looked at roundabouts built in Washington between 2009 and 2015, and found that crashes at double-lane roundabouts decreased at an average of 9% per year. Meanwhile, the odds of crashes at double-lane roundabouts involving severe injuries decreased by nearly one-thirds annually. In light of all these, the construction of double-lane roundabouts today is on the rise.

In order to study the performance of double-lane roundabouts, the creation of a comprehensive double-lane roundabout model is vital. One study conducted in 2000 highlights the importance of finding the most appropriate method for studying the capacity and performance of roundabouts in the United States [7]. All the methods used in this research had been proposed by other authors; the parameters are based on the traffic flow condition and geometric variation of roundabouts, but not the rate of density and flux changes. Another method is the so-called metering signals which is used to analyse the performance of roundabouts in terms of delays and queue length [8]. It is applied to the real-life scenario of unbalanced flow patterns. In this approach, the control parameters include the time for the traffic lights and the stop line setback distance. The density on the roundabout is not considered.

The Multi-stream Minimum Acceptable Space (MMAS) Cellular Automata (CA) model is also proposed to study double-lane roundabouts. This method only focuses on the junction at the entrance of the roundabout where the computation of traffic flow is on the "L" site which does not represent the intact double-lane roundabouts [9]. Capacity models have also been developed for single-lane and double-lane roundabouts; they are used to study double-lane roundabouts by separate entry lanes in 2009. This means that there are two different equations for studying the capacity of roundabouts. However, this method treats the double-lane roundabout as two different tubes with no interconnections between them. Furthermore, it does not represent the complete double-lane four-arm roundabout model; in other words, it only considers two separate lanes in a road [10].

In 2018, a double-lane roundabout model was derived interconnecting the inner and outer lane via a merge junction, diverge junction, and crossing junction [11]. However, it only considers the entry and exit on the junction. Despite the model's inner lane and outer lane interconnections, the computation of density on these two lanes is treated as a single lane; hence, it does not represent the double-lane four-arm roundabout model which is an essential aspect for studying its performance.

The model was developed from a single-lane roundabout model coupled with a waiting system [12, 13] and is a macroscopic model based on a hyperbolic partial differential equation.

2 Double-Lane Roundabout Model

In this research, the four-arm double-lane roundabout model is designed with two rings on the island of the roundabout where the traffic flow is in clockwise direction (see Figure 1).

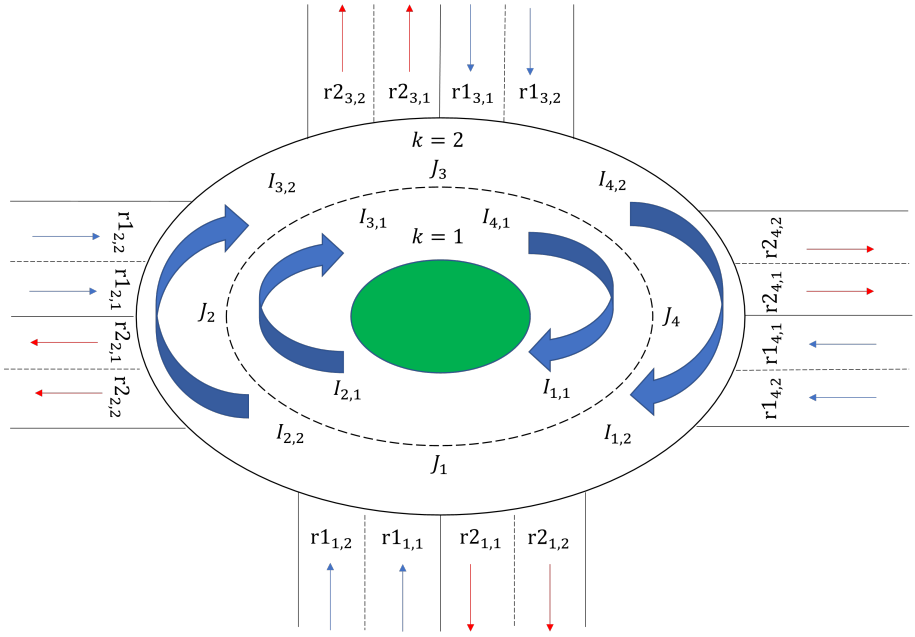

Figure 1: Roundabout Schematic

As shown in Figure 1, the smaller ring represents the inner lane and the larger ring represents the outer lane of the roundabout, denoted as $k = 1$ and $k = 2$, respectively. This is a four-arm double-lane roundabout whereby the arm junction is represented by $J_n,\ n = 1,\ 2,\ 3,\ 4$. The main lanes of the roundabout are labelled as $I_{n,\,k}$ where $n = 1,\ 2,\ 3,\ 4$ and $k = 1, 2$ in which each arm junction is depicted by an interval $[I_{n,\,k},\ I_{n+1,\,k}]$ for $n = 1,\ 2,\ 3,\ 4$ is $I_{5,\,k} = I_{1,\,k}$ that indicates the periodic boundary condition. Meanwhile, the secondary lanes consisting of both incoming and outgoing roads are labelled as $r1_{n,\,k}$ and $r2_{\,n,\,k}$ where $n = 1,\ 2,\ 3,\ 4$ and $k = 1, 2$.

The traffic flow on both inner and outer of the main lane segment is modified as

$$\partial_t \rho_{n,\,k} + \partial_x f(\rho_{n,\,k}) = 0, \quad (x,t) \in \mathbb{R}^+ \times I_{n,\,k},\ n = 1,\ 2,\ 3,\ 4 \text{ and } k = 1, 2 \tag{1}$$

With regards to Equation (1), $\rho_{n,\,k} = \rho_{n,\,k}(x,t) \in [0, \rho_{\max}]$ is the mean traffic density of which unit length $x \in \mathbb{R}$ at time $t \geq 0$, $\rho_{\max}$ is the maximal density whilst the flux function $f : [0, \rho_{\max}] \to \mathbb{R}^+$ is referred to the flux-density relation.

$$f(\rho) = \begin{cases} \rho v_{\max}, & 0 \leq \rho \leq \rho_c \\ \dfrac{f^{\max}}{\rho_{\max} - \rho_c}(\rho_{\max} - \rho), & \rho_c \leq \rho \leq \rho_{\max} \end{cases} \tag{2}$$

where $v_{\max}$ is the maximal traffic speed, $\rho_c = \dfrac{f^{\max}}{v_{\max}}$ is the critical density and $f^{\max} = f(\rho_c)$ is the maximal flux. To ensure that the simulation values remain within the range of $[0, 1]$,

both the maximum density and maximum traffic speed are normalized to one, represented as $\rho_{\max} = 1$ and $v_{\max} = 1$. For more details of Equation (2), the rational flux-density relation graph can be found in [12].

In order to accomplish the traffic flow on the whole roundabout, the flux from secondary lane entering the arm junction to outgoing main lane is assigned. On this account, the queue length of vehicles can be calculated and it is an ordinary differential equation.

$$\frac{dl_{n,k}(t)}{dt} = F_{\text{in}}^{n,k}(t) - \gamma_{\text{r1},n,k}(t), \quad t \in \mathbb{R}^+, \ n = 1,2,3,4 \text{ and } k = 1,2 \tag{3}$$

In Equation (3), $l_{n,k}(t) \in [0, +\infty]$ is the queue length on secondary lane, $F_{\text{in}}^{n,k}(t)$ is the flux entering the secondary lane and $\gamma_{\text{r1},n,k}(t)$ is the flux entering the roundabout from secondary lane.

Eventually, the Cauchy problem of the double-lane roundabout model is

$$\begin{cases} \partial_t \rho_{n,k} + \partial_x f(\rho_{n,k}) = 0, & (x,t) \in \mathbb{R}^+ \times I_{n,k} \\ \dfrac{dl_{n,k}(t)}{dt} = F_{\text{in}}^{n,k}(t) - \gamma_{\text{r1},n,k}(t), & t \in \mathbb{R}^+ \\ \rho_{n,k}(x,0) = \rho_{n,k,0}(x), & \text{on } I_{n,k} \\ l_{n,k}(0) = l_{n,k,0} \end{cases} \tag{4}$$

for $n = 1,\ 2,\ 3,\ 4$ and $k = 1,\ 2$ where $\rho_{n,k,0}(x)$ refers to the initial densities and $l_{n,k,0}$ is the initial queue length.

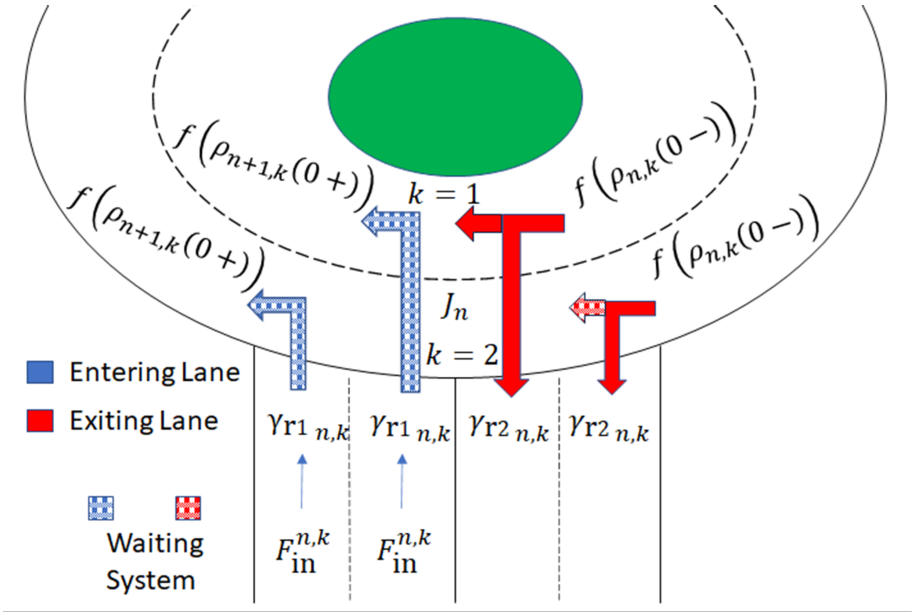

Figure 2: Traffic Flow at Arm Junction

Two fluxes demonstrate the traffic flow on arm junction are namely the incoming and outgoing flux. The flux from the incoming main lane is the sum of the flux of the outgoing main lanes and outgoing secondary lanes deducted by the flux of incoming secondary lanes as depicted in Figure 2.

$$f\left(\rho_{n,k}(0-,t)\right) = f\left(\rho_{n+1,k}(0+,t)\right) + \gamma_{r2n,k}(t) - \gamma_{r1n,k}(t) \tag{5}$$

where $n = 1, 2, 3, 4$ and $k = 1, 2$.

In Equation (5) above, the outgoing secondary lanes are represented as

$$\gamma_{r2n,k}(t) = \beta_{n,k} f\left(\rho_{n,k}(0-,t)\right) \tag{6}$$

where $\beta_{n,k} \in [0, 1]$ is the supply ratio of the outgoing secondary lanes $r2_{n,k}$ for $n = 1, 2, 3, 4$ and $k = 1, 2$.

Meanwhile, the flux of the inner and outer of outgoing main lanes is modified as

$$f\left(\rho_{n+1,k}(0+,t)\right) = \min\left((1-\beta_{n,k})\delta\left(\rho_{n,k}(0-,t)\right) + d\left(F_{in}^{n,k}(t), l_{n,k}(t)\right), \sigma\left(\rho_{n+1,k}(0+,t)\right)\right) \tag{7}$$

for $n = 1, 2, 3, 4$ and $k = 1, 2$.

To demonstrate the real phenomenon traffic flow on the roundabouts, some flux conditions on each of the arm junction are taken into consideration with the Cauchy problem in Equation (4) such as demand $d\left(F_{in}^{n,k}, l_{n,k}\right)$ on the inner and outer of the incoming secondary lanes, the demand function $\delta(\rho_{n,k})$ on the inner and outer of the incoming main lanes, and the supply function $\sigma(\rho_{n,k})$ on the inner and outer of the outgoing main lanes.

The proper regulation of traffic flow at the roundabout is that the cars from both inner and outer lanes of the incoming secondary lanes have to fully stop and ensure the clearance of cars from the incoming main lanes or existence of a certain safety gap on the arm junction of roundabout. Only then will the cars be permitted to enter the inner and outer lanes of the outgoing main lanes of roundabout. Consequently, the waiting system must be coupled with demand $d(F_{in}^{n,k}, l_{n,k})$ according to the conditions on the inner and outer lanes. Besides that, cars from the outer incoming main lane should also fully stop to let the cars from the inner incoming main lane to exit the roundabout. In this part, the demand function $\delta(\rho_{n,k})$ for $k = 2$ which is on the outer incoming lane must also be coupled with the waiting system. For the sake of coupling the waiting system, the computation of fluxes at the arm junction must be executed based on the Demand-limited case and Supply-limited case namely the Riemann solver of Riemann problem.

3 Riemann Problem and Riemann Solver

The Riemann problem at the arm junction, which corresponds to the Cauchy problem in Equation (4), is defined by the initial conditions $\rho_{n,k,0}(x) = \rho_{n,k,0}$ on $l_{n,k}$ and $l_{n,k}(0) = l_{n,k,0}$ for $n = 1, 2, 3, 4$ and $k = 1, 2$. This formulation describes each arm junction as having two incoming roads and two outgoing roads, located on the main lane and secondary lane of the roundabout. Furthermore, some parameters are fixed such as initial density $\rho_{n,k,0} \in [0, 1]$, initial queue length $l_{n,k,0} \in [0, \infty)$, flux entering the incoming roads on secondary lane, $F_{in}^{n,k} \in (0, \infty)$, priority factor $P_{n,k} \in (0, 1)$, and ratio splitting the outgoing lanes $\beta_{n,k} \in [0, 1]$. In this computation, the fluxes of inner and outer of the incoming main lane, $\Gamma_{n,k}^{t}$ and the fluxes of inner and outer entering

the roundabout from secondary lanes, $\Gamma^t_{r1,n,k}$ are computed. Referring to the part of Riemann Problem and Riemann Solver at Arm Junction in [12], the Riemann Solver depends on the fluxes of the outgoing main lane, $\Gamma^t_{2,n,k}$ and according to the demand-limited case or supply-limited case.

In both these cases, the flux of inner and outer of the incoming main lane is subjected to $\Gamma^t_{n,k} = f\left(\rho_{n,k}(0-,t)\right)$, meanwhile the flux of inner and outer of the outgoing main lane is described by $\Gamma^t_{2,n,k} = f\left(\rho_{n+1,k}(0+,t)\right)$ and the flux of inner and outer of the incoming secondary lane entering the roundabout $\Gamma^t_{r1,n,k} = \gamma_{r1,n,k}(t)$ are depicted as in Figure 2.

4 Computation of Flux and Number of Cars

Since $\Gamma^t_{1n,k}$ is the flux of inner and outer of the incoming main lane, therefore the both inner and outer flux coming from the incoming main lane then crossing the arm junction and heading to the outgoing main lane can be computed by

$$(1-\beta_{n,k})\,\Gamma^t_{n,k} \tag{8}$$

Meanwhile, the total number of cars crossing the arm junction $N_{\mathrm{car}\gamma^t_{n,k}}$ can be calculated by

$$N_{\mathrm{car}\gamma^t_{n,k}} = \int_t^{t+1} (1-\beta_{n,k})\Gamma^t_{n,k}\,dt \tag{9}$$

As Equation (8) represents the flux passing through the arm junction and heading to the outgoing main lane from the incoming main lane, hence, flux exiting the roundabout from the inner of incoming main lane is

$$(\beta_{n,1})\Gamma^t_{n,1} \tag{10}$$

and the total number of cars exiting the roundabout $N_{\mathrm{car}\psi^t_{n,1}}$ can be calculated by

$$N_{\mathrm{car}\psi^t_{n,1}} = \int_t^{t+1} (\beta_{n,1})\Gamma^t_{n,1}\,dt \tag{11}$$

5 The Coupling of Waiting System

5.1 Triggering of Waiting System

The objective of triggering the waiting system is to pause the cars to avoid collision with other cars that have priority to pass through. Additionally, as mentioned, the proper traffic flow on roundabouts as shown in Figure 2, cars from both inner and outer of the incoming secondary lane have to fully stop to make sure an existence of safety gap with the cars from incoming main before entering the roundabout. This is the reason for computing the flux and number of cars at the incoming main lane as presented in Section 4.1. Meanwhile, the cars from the outer of the incoming main lane to the outer of the outgoing main lane via arm junction crossing must also fully stop if there are exiting cars from the inner of the incoming main lane as they have the precedence to exit the roundabout. Thus, the waiting system must be incorporated

with the flux from the outer of the incoming main lane to the outer of the incoming main lane as described in Section 4.2.

The triggering of the waiting system $T_{n,k}^t$ is

$$T_{n,k}^t = \begin{cases} \text{Off} & ; \text{Ncar}_{n,k}^t \in [0, 0.5) \\ \text{On} & ; \text{Ncar}_{n,k}^t \in [0.5, 1] \end{cases} \tag{12}$$

In Equation (12), the activation of triggering of the 'On' and 'Off' modes is referred to the computation of the number of cars in Equation (9) and Equation (11). Note that the computation of the number of cars entails the accumulation of the integration of flux. Therefore, the decimal number of cars represents the cars approaching the arm junction. When the number of cars is 1, it means that the car has reached and crossed the arm junction. Furthermore, when the number of cars is between 0 and 0.5, it indicates that the gap between a vehicle on the incoming main lane and the arm junction is sufficiently large. When the total number of cars is between 0.5 and 1, it implies that a vehicle from the incoming main lane is approaching the arm junction. For more details about the operational of waiting system, it is in [13].

5.2 The Procedures of the Coupling of Waiting System

Because of the cars from both inner and outer of the incoming secondary lane have to fully stop to allow the cars from both inner and outer of the incoming main lane to pass through the arm junction to the outgoing main lane. Therefore, the flux on both inner and outer of the incoming secondary lane needs to be coupled with the waiting system to describe the mentioned phenomenon and it breaks down to two conditions of coupling with the waiting system on the inner and outer of the incoming secondary lane as shown in Figure 2.

5.2.1 Inner of the Incoming Secondary Lanes

The cars on the inner of the incoming secondary lane must ensure clearance from the inner and outer of the incoming main lane before they are allowed to enter the inner of the outgoing main lane of the roundabout. Hence, the triggering of the waiting system on the inner of the incoming secondary lane needs to take into account the cars on both the inner and outer of the incoming main lane. Based on Equation (12), the triggering of the waiting system on the inner of the incoming secondary lanes is

$$T_{n,1}^t = \begin{cases} \text{Off} & ; \quad 0 \leq \text{Ncar}_{\gamma_{n,1}}^t < 0.5 \text{ and } 0 \leq \text{Ncar}_{\gamma_{n,2}}^t < 0.5 \\ \text{On} & ; \quad 0 \leq \text{Ncar}_{\gamma_{n,1}}^t < 0.5 \text{ and } 0.5 \leq \text{Ncar}_{\gamma_{n,2}}^t \leq 1 \\ \text{On} & ; \quad 0.5 \leq \text{Ncar}_{\gamma_{n,1}}^t \leq 1 \text{ and } 0 \leq \text{Ncar}_{\gamma_{n,2}}^t \leq 0.5 \end{cases} \tag{13}$$

where $n = 1, 2, 3, 4$.

5.2.2 Outer of the Incoming Secondary Lanes

On the outer of the incoming secondary lane, the cars only need to ensure clearance from the outer of the incoming main lane before they are allowed to enter the outer of the outgoing main lane of the roundabout. Thus, the triggering of the waiting system on the outer of the incoming secondary lane only needs to consider the cars on the outer of the incoming main lane.

$$T_{in,2}^{t} = \begin{cases} 0 & ; \quad 0 \leq N\text{carry}_{n,2}^{t} < 0.5 \text{ and } 0 \leq N\text{carry}_{n,2}^{t} < 0 \\ \text{On}, & ; \quad 0 \leq N\text{carry}_{n,2}^{t} < 0.5 \text{ and } 0.5 \leq N\text{carry}_{n,2}^{t} \geq 1 \\ \text{On}, & ; \quad 0.5 \leq N\text{carry}_{n,2}^{t} < 1 \text{ and } 0 \leq N\text{carry}_{n,2}^{t} \geq 0.5 \end{cases} \tag{14}$$

where $n = 1, 2, 3, 4$.

Next, the triggering of the waiting systems as in Equation (13) and Equation (14) need to be incorporated with the demand in Equation (7), thus yielding

$$d(F_{in}^{n,k}, l_{n,k}) = \begin{cases} 0 & ; \quad T_{in,k}^{t} = 0 \text{ on} \\ \gamma_{\max}^{r1,n,k} & ; \quad T_{in,k}^{t} = 0 \text{ off and } l_{n,k}(t) > 0 \\ \min(F_{in}^{n,k}(t), \gamma_{\max}^{r1,n,k}) & ; \quad T_{in,k}^{t} = 0 \text{ off and } l_{n,k}(t) = 0 \end{cases} \tag{15}$$

where $\gamma_{\max}^{r1,n,k}$ is the maximal flux entering the roundabout from the incoming secondary lane for $n = 1, 2, 3, 4$ and $k = 1, 2$.

Another waiting system that needs to be coupled with is on the outer of the incoming main lanes to the outer of the outgoing main lanes by crossing the arm junction. This is to allow the cars from the inner of the incoming main lanes to exit the roundabout as shown in Figure 2. In other words, the demand function on the inner of the incoming main lanes does not require the waiting system.

5.2.3 Inner of the Incoming Main Lanes

The cars from the inner of the incoming main lanes have priority to exit the roundabout, hence it does not need the waiting system.

$$\delta(\rho_{n,k}) = \begin{cases} f(\rho_{n,k}), & 0 \leq \rho_{n,k} < \rho_c \\ f^{\max}, & \rho_c \leq \rho_{n,k} \leq 1 \end{cases} \tag{16}$$

where $n = 1,\ 2,\ 3,\ 4$ and $k = 1$.

5.2.4 Outer of the Incoming Main Lanes

The cars on the outer of the incoming main lanes need to pause to give way to the cars from the inner of the incoming main lanes to exit the roundabout. Therefore, the computation of flux and number of cars on the inner of the incoming main lanes are based on Equation (10) and Equation (11), respectively, as shown in Section 4.2. Next, Equation (12) is incorporated with the demand function, thus yielding

$$\delta(\rho_{n,k}) = \begin{cases} 0, & T_{n,k}^{t} = \text{On} \\ f(\rho_{n,k}), & T_{n,k}^{t} = \text{Off and } 0 \leq \rho_{n,k} < \rho_c \\ f^{\max}, & T_{n,k}^{t} = \text{Off and } \rho_c \leq \rho_{n,k} \leq 1 \end{cases} \tag{17}$$

where $n = 1,\ 2,\ 3,\ 4$ and $k = 2$.

Lastly, with regards to the intact of traffic flow at arm junction, the supply function on the inner and outer of the outgoing main lanes is

$$\sigma(\rho_{n,k}) = \begin{cases} f^{\max}, & 0 \leq \rho_{n,k} \leq \rho_c \\ f(\rho_{n,k}), & \rho_c < \rho_{n,k} \leq 1 \end{cases} \tag{18}$$

where $n = 1,\ 2,\ 3,\ 4$ and $k = 1,\ 2$.

6 Network Topology

Notice that the main lane of the four-arm roundabout is namely by $I_{n,k}$ for $n = 1, 2, 3, 4$ and $k = 1, 2$. The both inner and outer lanes of main lane of the double-lane roundabout is divided equally by i node points and configures the number of intervals $(i + 1)$. In addition, secondary lane associates to each arm junction with two incoming lanes and two outgoing lanes, specifically the inner lane and outer lane. The restrictions of the traffic flow on roundabout are unsignalized and no overtaking of cars.

6.1 Numerical Scheme

Based on the defined topology, the numerical grid is specified over the domain $J_n \leq x \leq J_{n+1}$ and $0 \leq t \leq T$, with the following notation adopted:

- Δx is the space grid size.
- Δt^j is the inconstant time grid size.
- $(x_{i,k},\ t^j) = (i\Delta x,\ t^{j-1} + \Delta t^j)$ for $i \in \mathbb{Z}$, $j \in \mathbb{N}$ and $k = 1,\ 2$ are the grid points.

6.2 The Courant-Friedrichs-Lewy (CFL) Condition

The model is a hyperbolic partial differential equation and is classified as a wave equation. Therefore, convergent solutions are necessary for solving this equation. In order to obtain the convergent solutions, the Δt^j can be determined by CFL condition which is

$$\Delta t^j \max \left| \lambda^j_{i+\frac{1}{2}h,\ k} \right| \leq \frac{1}{2}\Delta x, \quad \text{where } i \in \mathbb{Z},\ j \in \mathbb{N} \text{ and } k = 1, 2, \tag{19}$$

where $\left| \lambda^j_{i+\frac{1}{2}h,\ k} \right|$ is absolute value of the wave speed at the interface $x_{i+\frac{1}{2}h}$ at time t^j and it is the derivative of flux-density relation in Equation (2) $f'(u)$. Meanwhile, h denotes the space step size.

6.3 Godunov Method

The Godunov method is used to exactly compute the flux at each cell interface for solving the Riemann problem. The details and derivation of solutions using the Godunov method can be referred to [12].

The density at the non-arm junction nodes can be computed by

$$u_{i,k}^{j+1} = u_{i,k}^{j} - \frac{\Delta t^j}{\Delta x}\left(G(u_{i,k}^{j}, u_{i+1,k}^{j}) - G(u_{i-1,k}^{j}, u_{i,k}^{j})\right) \tag{20}$$

where $G(u_{i,k}^{j}, u_{i+1,k}^{j}) = G_{i+\frac{1}{2},k}^{j}$ is the Godunov numerical flux computed by Equation (23) in [12]. At arm junction, the density of the incoming main lanes is written as

$$u_{i,k}^{j+1} = u_{i,k}^{j} - \frac{\Delta t^j}{\Delta x}\left(\Gamma_{1\ n,k}^{j} - G(u_{i-1,k}^{j}, u_{i,k}^{j})\right) \tag{21}$$

while the density of the outgoing main lanes is

$$u_{i,k}^{j+1} = u_{i,k}^{j} - \frac{\Delta t^j}{\Delta x}\left(G(u_{i,k}^{j}, u_{i+1,k}^{j}) - \Gamma_{2\ n,k}^{j}\right) \tag{22}$$

where $\Gamma_{1\ n,k}^{j}$ and $\Gamma_{2\ n,k}^{j}$ are the maximised fluxes computed at time t^j representing the fluxes on the incoming main lanes and outgoing main lanes, respectively, which in Section 3 are explained as the Riemann Problem and Riemann Solver.

6.4 Queue Length on Secondary Lanes

There are two possible cases for the buffer modelled in Equation (3).

- For $F_{\text{in}}(t^j) < \Gamma_{\text{r1}}^{j,n,k}$

$$l_{n,k}^{j+1} = \begin{cases} l_{n,k}^{j} + \left(F_{\text{in}}^{n,k}(t^j) - \Gamma_{\text{r1}}^{j,n,k}\right)\Delta t^j, & t^{j+1} < \bar{t}_{n,k}^{j} \\ 0, & \text{otherwise} \end{cases} \tag{23}$$

- For $F_{\text{in}}(t^j) > \Gamma_{\text{r1}}^{j,n,k}$

$$l_{n,k}^{j+1} = l_{n,k}^{j} + \left(F_{\text{in}}^{n,k}\left(t^j\right) - \Gamma_{\text{r1}}^{j,n,k}\right)\Delta t^j \tag{24}$$

where $\Gamma_{\text{r1}}^{j,n,k}$ is the maximised flux computed at time t^j representing the flux entering the roundabout from the incoming of the secondary lanes, which in Section 3 is explained as the Riemann Problem and Riemann Solver. In addition, the $\bar{t}_{n,k}^{j}$ in Equation (23) is given by

$$\bar{t}_{n,k}^{j} = -\frac{l_{n,k}^{j}}{F_{\text{in}}^{n,k}(t^j) - \Gamma_{\text{r1}}^{j,n,k}} + t^j \tag{25}$$

for $t^j = t^{j-1} + \Delta t^j$.

7 Simulation Settings

In the simulation, specific parameters are prescribed under certain assumptions to realistically represent traffic flow such as $F_{\text{in}}^{n,k} \in [0,1]$, $\beta_{n,k} \in [0,1]$, and $P_{n,k} \in [0,1]$ where $n = 1,2,3,4$ and $k = 1,2$. Two initial conditions are needed: $\rho_{n,k,0} = 0$ and $l_{n,k,0} = 0$ where $n = 1,2,3,4$ and $k = 1,2$. Furthermore, some constants are fixed such as maximal flux $f^{\max} = 0.66$, critical density $\rho_c = 0.66$ and maximal flow on the incoming secondary lanes $\gamma_{\text{r1}}^{\max} = 0.65$. The total time and space step are $T = 10$ and $\Delta x = 0.1$, respectively. In terms of the dimension of the roundabout, the circumference of the inner and outer of roundabout are set to be same which is four-unit lengths. The parameter settings of the four simulations are presented in Table 1 until Table 4 below.

Table 1: Parameter settings for Simulation 1

Parameter	**Values**
F_{in}	0.2, 0.4, 0.6, 0.8, 1.0
P	0.3, 0.5, 0.8
$\beta_{n,1}$	0.4 (for $n = 1,\ 2,\ 3,\ 4$)
$\beta_{n,2}$	0.6 (for $n = 1,\ 2,\ 3,\ 4$)

Table 2: Parameter settings for Simulation 2

Parameter	**Values**
F_{in}	0.2, 0.4, 0.6, 0.8, 1.0
P	0.3, 0.5, 0.8
$\beta_{n,1}$	0.6 (for $n = 1,\ 2,\ 3,\ 4$)
$\beta_{n,2}$	0.8 (for $n = 1,\ 2,\ 3,\ 4$)

8 Optimizations

In logical and reasonableness analysis, the computations of Total Travel Time (TTT) on the road network and Total Waiting Time (TWT) at the entrance of the secondary road are modified from [12], though, the computed data are non-unit of measurement.

$$\text{TTT}_k = \sum_k \sum_{n=1}^{N} \int_0^T \int_{I_{n,k}} \rho(x,t)\,dx\,dt + \sum_k \sum_{n=1}^{N} \int_0^T l_{n,k}(t)\,dt + T \cdot \sum_k \sum_{n=1}^{N} l_{n,k}(T) \tag{26}$$

$$\text{TWT}_k = \sum_k \sum_{n=1}^{N} \int_0^T l_{n,k}(t)\,dt + T \cdot \sum_k \sum_{n=1}^{N} l_{n,k}(T) \tag{27}$$

where T is total time, N is the number of arms, $n = 1,2,3,4$ and $k = 1,2$.

Table 3: Parameter settings for Simulation 3

Parameter	**Values**
F_{in}	0.2, 0.4, 0.6, 0.8, 1.0
P	0.3, 0.5, 0.8
$\beta_{n,1}$	0.5 (for $n = 1,\ 2,\ 3,\ 4$)
$\beta_{n,2}$	0.5 (for $n = 1,\ 2,\ 3,\ 4$)

Table 4: Parameter settings for Simulation 4

n	$F_{\text{in}}^{n,1}$	$F_{\text{in}}^{n,2}$	$P_{n,1}$	$P_{n,2}$	$\beta_{n,1}$	$\beta_{n,2}$
1	0.4	0.7	0.5	0.3	0.3	0.6
2	0.6	0.2	0.2	0.1	0.2	0.8
3	0.3	0.8	0.4	0.2	0.3	0.7
4	0.9	0.2	0.3	0.2	0.4	0.9

Furthermore, to study the efficiency of roundabouts in terms of time consumption and queue length, the differences of the TTT, TWT and queue length between the simulations must be calculated and the notations are as follows.

$$\text{TTT}_k^D = \frac{\text{TTT}_k^{\mathcal{S}} - \text{TTT}_k^s}{\text{TTT}_k^s} \times 100\% \tag{28}$$

$$\text{TWT}_k^D = \frac{\text{TWT}_k^{\mathcal{S}} - \text{TWT}_k^s}{\text{TWT}_k^s} \times 100\% \tag{29}$$

$$l_{n,k}^D = \frac{l_{n,k}^{\mathcal{S}} - l_{n,k}^s}{l_{n,k}^s} \times 100\% \tag{30}$$

where $n = 1,\ 2,\ 3,\ 4$, $k = 1,\ 2$, $\mathcal{S}$ is the new component and s is the old component.

9 Result and Discussion

According to the setting of the simulation, the value of β for the outer lane is higher than that of the inner lane as it indicates the realistic phenomenon whereby most of the vehicles in the outer lane will exit the roundabout at the next exit; however, the vehicles in the inner lane will circulate the roundabout to exit the second, third, or fourth exit. This differentiation in β directly influences the distribution of density and flux between two lanes. In the first three simulations, the graphs of F_{in} versus TTT, F_{in} versus TWT, and F_{in} versus queue length are plotted. These results show the reasonableness and logical simulations as the F_{in} increases when the TTT, TWT, and queue length increase, consistent with congestion formation in macroscopic traffic models. From Figure 3 to Figure 8 with the increasing value of P, a jam occurs on the main lane and secondary lane of the roundabout. Thus, the waiting system is

activated where the case of $P = 0.8$ shows the lowest TTT and highest TWT. On the contrary, the case of $P = 0.3$ shows the highest TTT and lowest TWT, as lower F_{in} prolongs circulation time while reducing queuing at entry. In Simulation 1, the sharp growth of both TTT and TWT with increasing of F_{in} indicates a strong sensitivity to lane interactions. The higher β on the outer lane drives earlier exits, but this induces repeated merging and diverging processes at the junctions, amplifying local density fluctuations and queue formation. In Simulation 2, although the outer lane β is set higher at 0.8, the growth of TTT and TWT with increasing F_{in} is noticeably less sharp compared to Simulation 1. This is because a larger proportion of vehicles exit the roundabout earlier, which reduces the circulation load within the inner parts of the roundabout. As a result, congestion does not accumulate as heavily inside the system, and the increase in travel and waiting times becomes more gradual. In effect, the higher β value improves the flushing of vehicles through the roundabout, preventing severe buildup even under rising F_{in} rates. While the merge zones still experience stress at higher F_{in}, the continuous exit of vehicles allows the system to reset more frequently, thereby smoothing the overall trend of TTT and TWT compared to the sharper curves observed in Simulation 1.

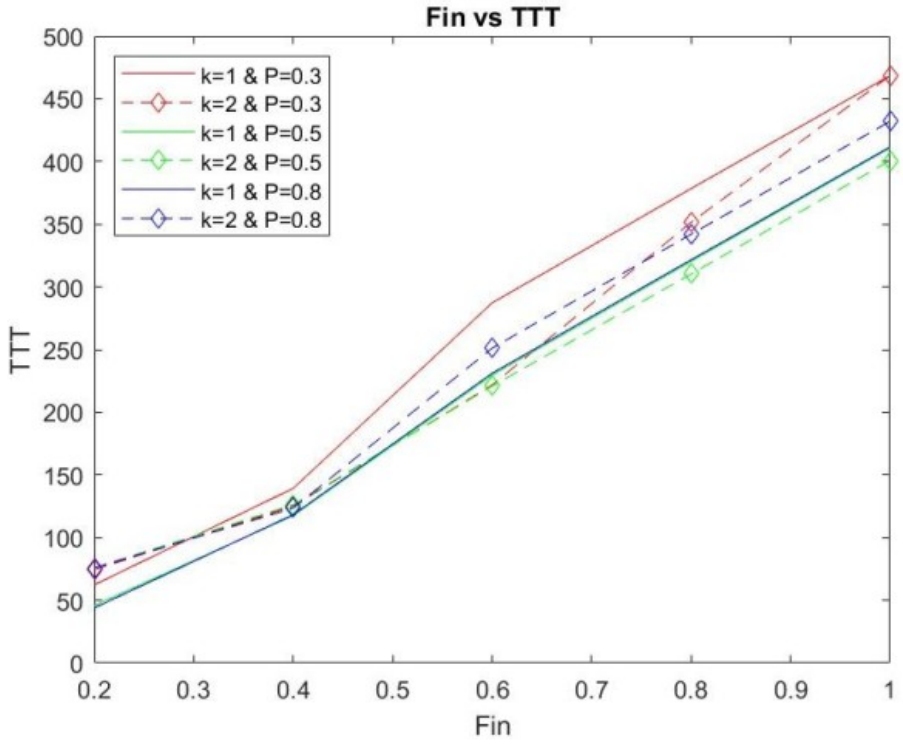

Figure 3: F_{in} versus TTT in Simulation 1

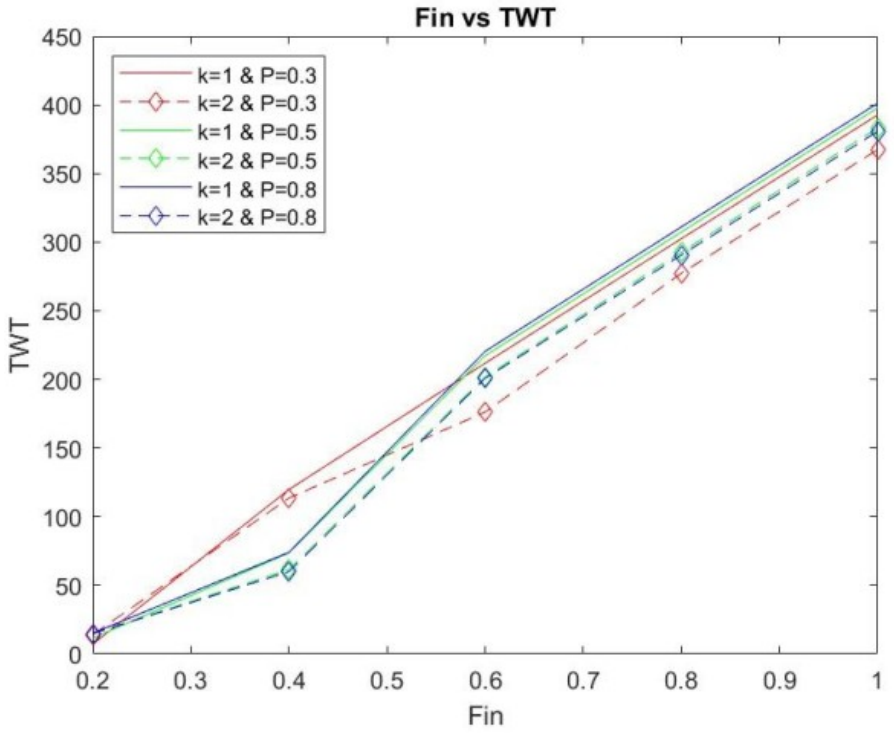

Figure 4: F_{in} versus TWT in Simulation 1

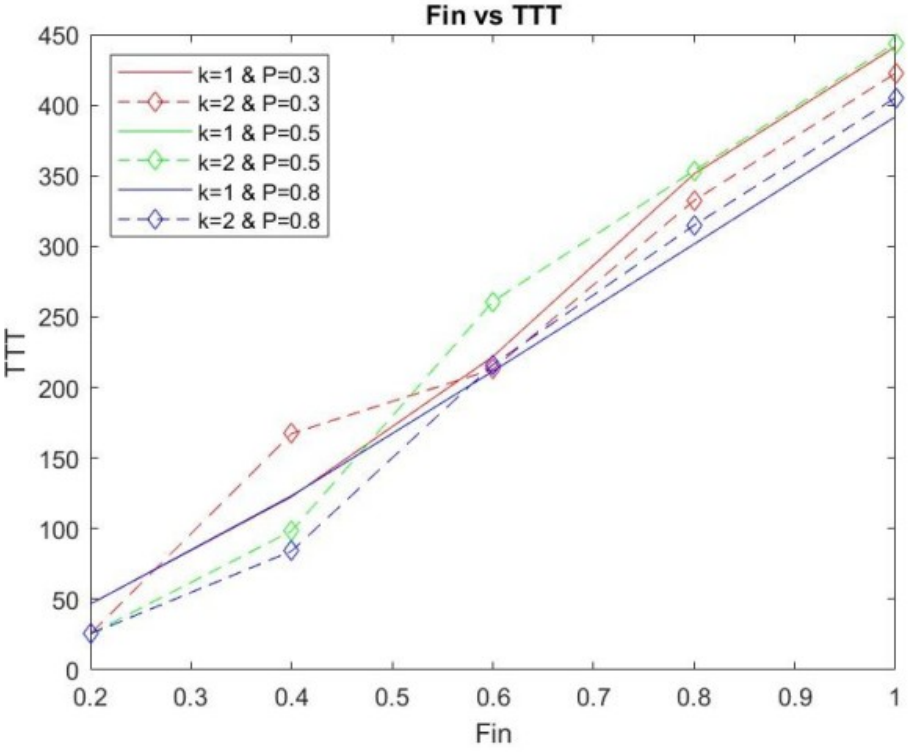

Figure 5: F_{in} versus TTT in Simulation 2

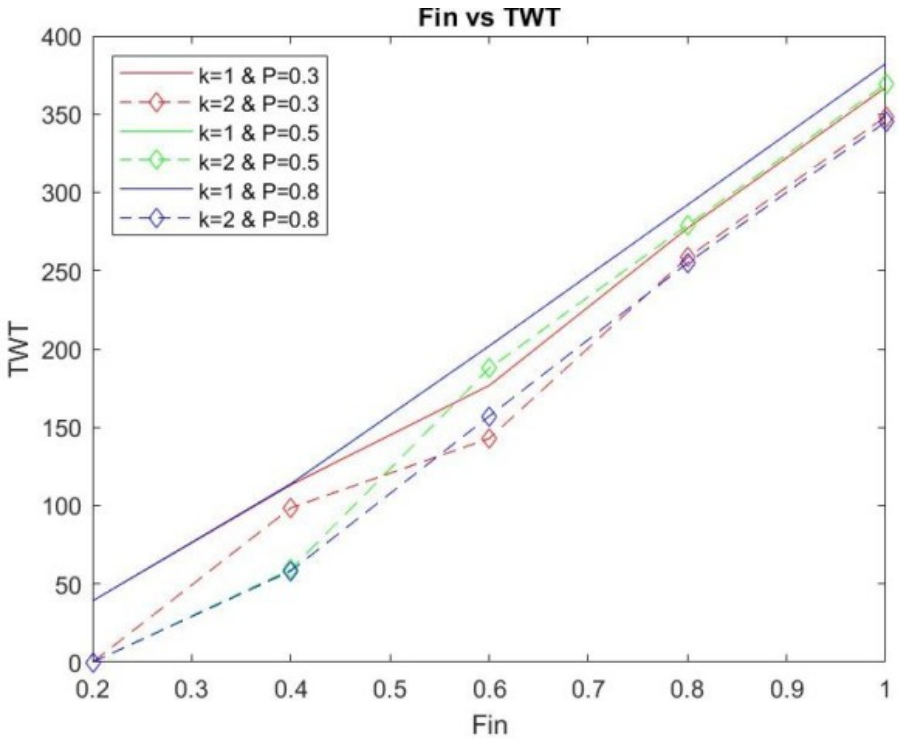

Figure 6: F_{in} versus TWT in Simulation 2

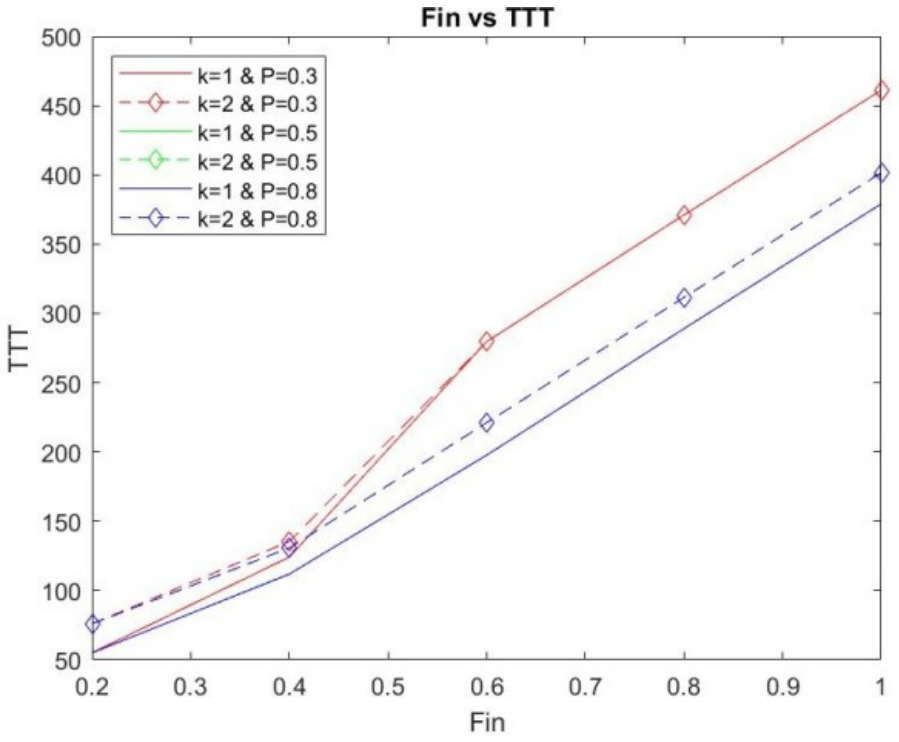

Figure 7: F_{in} versus TTT in Simulation 3

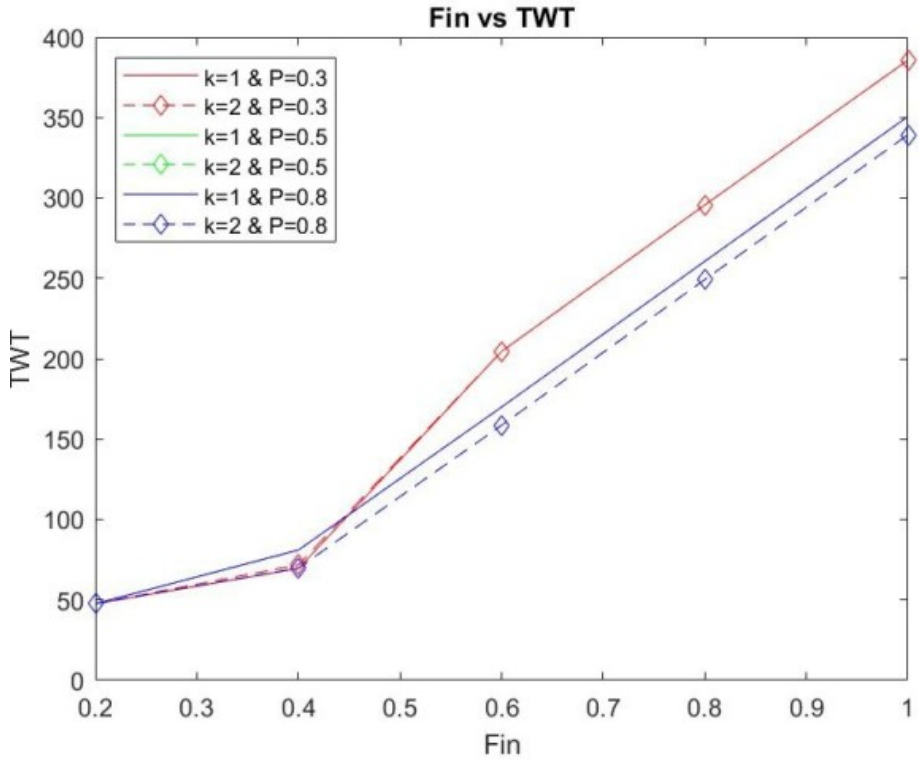

Figure 8: F_{in} versus TWT in Simulation 3

In Figure 5 and Figure 6, the outer lane of the case of $P = 0.8$ shows the lowest TWT. This is because the values of β and P are high, indicating that most of the vehicles exit the roundabout at the next exit, reducing waiting. However, this early exit behaviour shifts more pressure onto the incoming lane, which explains why TTT remains higher despite the reduction in TWT.

In Simulation 3, the value of β is set to be the same on the inner lane and outer lane namely 0.5. Therefore, both the inner lane and outer lane shown in Figure 7 and Figure 8 are overlapped, demonstrating balanced utilization of capacity. The only difference is with case $P = 0.8$ between the inner lane and outer lane whereby the incident is similar to the incident in Figure 6. Consequently, the TTT for the outer lane is higher than that of the inner lane whereas the TWT for the outer lane is lower than that of the inner lane as shown in Figure 7 and Figure 8. This asymmetry arises because increased F_{in} combined with balanced β produces a denser circulation in the outer lane, while the inner lane absorbs more queuing. Overall, Simulation 3 yields the most stable growth patterns of TTT and TWT, confirming that parameter symmetry leads to smoother macroscopic behavior.

According to Figure 4 and Figure 6, the TWT for case $P = 0.8$ is the highest out of all the other cases. It also reflects the longest queue length on the secondary lane of the roundabout, as depicted in Figure 9 and Figure 10, because even though higher F_{in} reduces TTT through faster circulation, it simultaneously intensifies local bottlenecks. On the other hand, the case of $P = 0.3$ shows the shortest queue length due to it having the highest TTT, as shown in Figure 3 and Figure 5, because vehicles remain in circulation longer, spreading density around the roundabout and lowering localized waiting.

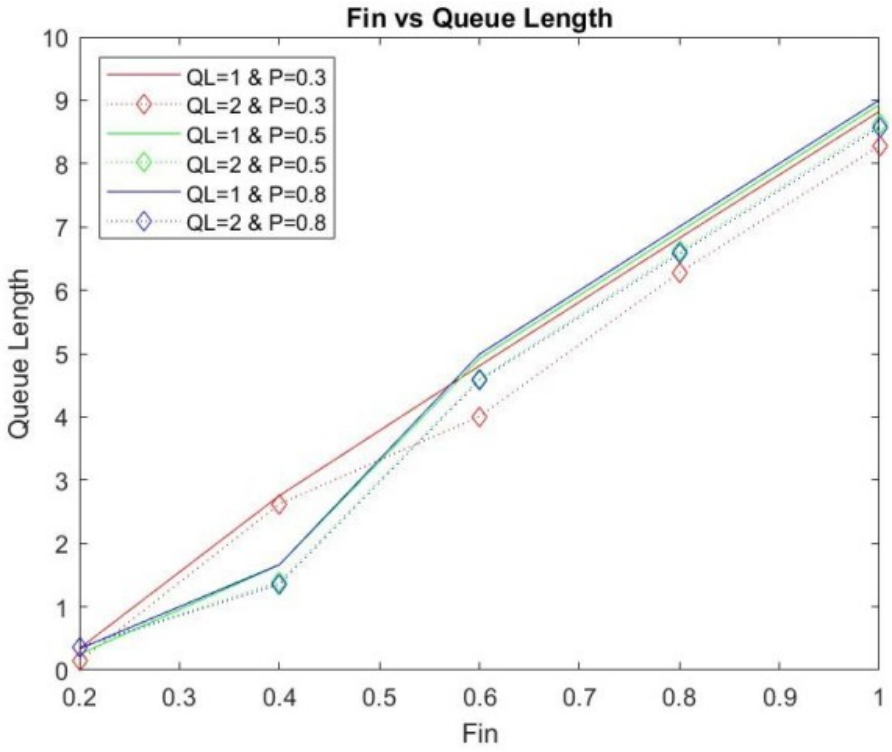

Figure 9: F_{in} versus Queue Length in Simulation 1

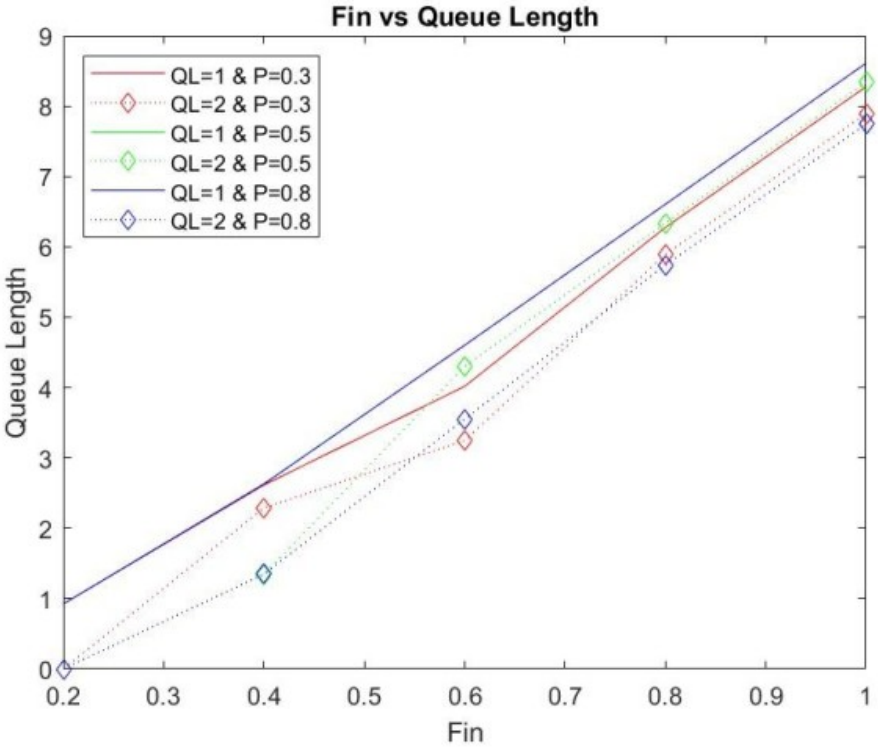

Figure 10: F_{in} versus Queue Length in Simulation 2

In Simulation 3, the inner lane and outer lane have the same value of β, and hence the same queue length. In the case of $P = 0.8$ as shown in Figure 7 and Figure 8, the TTT on the outer lane is higher than that on the inner lane whereas the TWT on the outer lane is lower than that on the inner lane, thus yielding longer queue length on the inner lane than on the outer lane. In Figure 11, equal β values lead to identical queue lengths in both lanes under most cases. Under $P = 0.8$, however, the higher TTT in the outer lane and the higher TWT in the inner lane translate into longer queues in the inner lane, demonstrating a redistribution of congestion rather than a reduction.

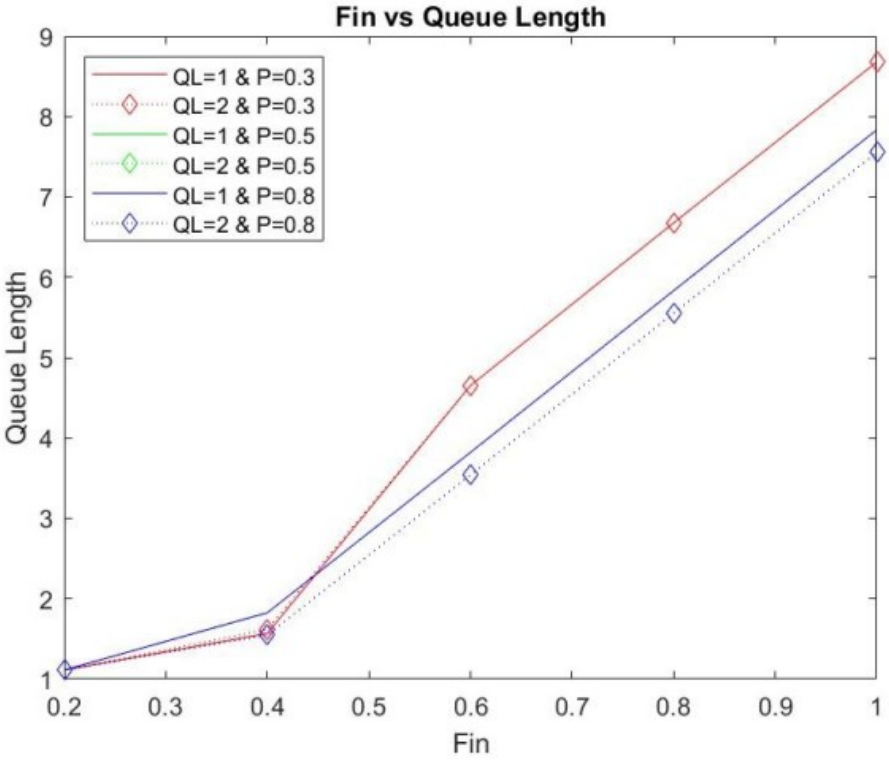

Figure 11: F_{in} versus Queue Length in Simulation 3

As shown in Simulation 4, this model is designed with a distinct entry parameter at each junction, inner lane, and outer lane, introducing spatial heterogeneity. Referring to the results in Figure 12 the inner lane of the fourth junction has the longest tailback as the flux entering the secondary lane is high. However, the crossing rate at the arm junction and the exiting rate at the roundabout at the inner lane of the first junction are low. On the other hand, the outer lane of the fourth junction has the shorter queue length, even though the crossing rate at the arm junction is low. The flux entering the secondary lane is also low whilst the exiting rate at the roundabout at the inner lane of the first junction is high. Hence, no congestion occurs on the outer lane of the fourth junction. This parameter heterogeneity produces localized congestion differences, as seen in the computed TTT and TWT values on the inner lane and outer lane are 273.57 and 99.21, and 201.46 and 82.6107, respectively. These findings demonstrate that inflow distribution, exit probability, and lane-specific flux interactions are critical determinants of double-lane roundabout performance.

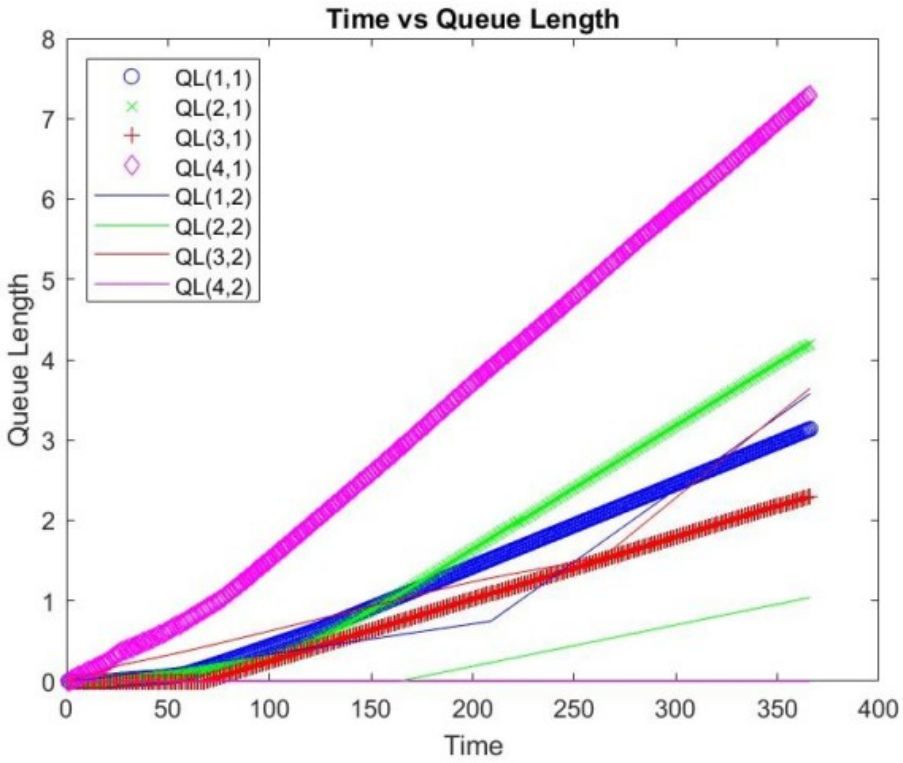

Figure 12: Time versus Queue Length in Simulation 4

Table 5 and Table 6 show the percentage differences in TTT and TWT, as well as queue length between Simulation 1 and Simulation 2 were computed using Equations (28) to (30), based on the parameter settings in Tables 1 and 2. In both simulations, the flux entering the secondary lane, F_{in} and priority factor, P were kept the same, while the main difference lay in the supply ratio of the outgoing secondary lanes, β. Specifically, Simulation 1 used $\beta_{n,1} = 0.4$ and $\beta_{n,2} = 0.6$, whereas Simulation 2 used higher exit rate of $\beta_{n,1} = 0.6$ and $\beta_{n,2} = 0.8$. This difference implies that vehicles in Simulation 2 were more likely to exit the roundabout earlier, which is expected to reduce both TTT and TWT compared to Simulation 1.

The results in Table 5 confirm this expectation, showing that Simulation 2 generally yields lower TTT as negative percentages of TTT^D, across most the flux entering the secondary lane rates. At very low rate, $F_{\text{in}} = 0.2$, Simulation 2 dramatically reduces TTT compared to Simulation 1, with reductions of up to 65%. At moderate rates, F_{in} equals 0.4 and 0.6, the results are more balanced, with Simulation 2 reducing TTT while TWT shows mixed but smaller deviations. At high rates, F_{in} equals 0.8 and 1.0, Simulation 2 consistently reduces both TTT and TWT, suggesting improved efficiency under heavier traffic conditions.

Table 5: The difference in TTT and TWT between Simulation 1 and Simulation 2

P	0.3				0.5				0.8			
F_{in}	TTT_1^D (%)	TTT_2^D (%)	TWT_1^D (%)	TWT_2^D (%)	TTT_1^D (%)	TTT_2^D (%)	TWT_1^D (%)	TWT_2^D (%)	TTT_1^D (%)	TTT_2^D (%)	TWT_1^D (%)	TWT_2^D (%)
0.2	-25.31	-65.88	447.82	-100.00	1.52	-66.48	238.93	-100.00	6.02	-66.48	159.83	-100.00
0.4	-12.00	33.61	-5.43	-13.19	4.93	-22.10	54.80	-3.70	4.14	-31.95	53.84	-2.75
0.6	-22.78	-4.00	-16.60	-18.95	-7.93	18.07	-7.04	-7.07	-8.50	-13.94	-8.40	-21.75
0.8	-7.17	-5.42	-8.40	-6.78	-5.86	13.93	-4.99	-4.65	-6.22	-7.92	-6.12	-12.30
1.0	-5.80	-9.82	-6.49	-5.13	-4.62	10.74	-3.90	-3.60	-4.81	-6.22	-4.70	-9.34

Table 6: The difference in queue length between Simulation 1 and Simulation 2

P		0.3				0.5				0.8			
F_{in}	$l^D_{n,k}$ (%)	$n=1$	$n=2$	$n=3$	$n=4$	$n=1$	$n=2$	$n=3$	$n=4$	$n=1$	$n=2$	$n=3$	$n=4$
0.2	$k=1$	172.08	172.08	172.08	172.08	269.77	269.77	269.77	269.77	175.81	175.81	175.81	175.81
	$k=2$	-100	-100	-100	-100	-100	-100	-100	-100	-100	-100	-100	-100
0.4	$k=1$	-5.02	-5.02	-5.02	-5.02	58.33	58.33	58.33	58.33	57.92	57.92	57.92	57.92
	$k=2$	-12.68	-12.68	-12.68	-12.68	-3.58	-3.58	-3.58	-3.58	-0.44	-0.44	-0.44	-0.44
0.6	$k=1$	-16.43	-16.43	-16.43	-16.43	-6.50	-6.50	-6.50	-6.50	-7.78	-7.78	-7.78	-7.78
	$k=2$	-18.97	-18.97	-18.97	-18.97	-6.50	-6.50	-6.50	-6.50	-22.39	-22.39	-22.39	-22.39
0.8	$k=1$	-8.05	-8.05	-8.05	-8.05	-4.61	-4.61	-4.61	-4.61	-5.69	-5.69	-5.69	-5.69
	$k=2$	-6.15	-6.15	-6.15	-6.15	-4.27	-4.27	-4.27	-4.27	-12.73	-12.73	-12.73	-12.73
1.0	$k=1$	-5.80	-9.82	-6.49	-5.13	-4.62	10.74	-3.90	-3.60	-4.81	-6.22	-4.70	-9.34
	$k=2$	-4.67	-4.67	-4.67	-4.67	-3.32	-3.32	-3.32	-3.32	-9.71	-9.71	-9.71	-9.71

Table 6 provides further insight into queue lengths. At low rates of F_{in}, Simulation 2 results in much longer queues in inner lane by increasing of over 170% to 270%, while outer lane queues are completely eliminated which is −100%. At medium rates of F_{in}, the differences in queue length become predominantly negative with −5% to −20%, indicating that Simulation 2 reduces congestion more evenly across lanes. At higher rates of F_{in}, the improvements remain but are smaller in magnitude, with reductions in queue length typically between −5% and −10%. Overall, the comparison demonstrates that Simulation 2, with higher exit probabilities, achieves greater efficiency by lowering travel time and, in most cases, reducing queue lengths compared to Simulation 1.

10 Conlusion

Based on the results presented above, it can be concluded that the double-lane roundabout model has been created successfully, with the waiting system playing a vital role in representing real traffic flow. This model incorporates multiple entry parameters that allow for detailed study of traffic performance at roundabouts. Although the data do not reflect actual empirical observations, the variations in increasing and decreasing trends provide meaningful insights into traffic dynamics. Compared with existing models, which either rely solely on geometric variations without density and flux [7], focus only on delays and queues [8], limit analysis to entrance junctions [9], or treat double-lane roundabouts as disconnected single lanes [10,11], the proposed model overcomes these shortcomings by representing the full four-arm double-lane roundabout with density and flux dynamics. Consequently, this model not only advances the accuracy of roundabout performance analysis but also proves beneficial for researchers, as well as government and private agencies involved in traffic management and planning.

Acknowledgments

This work was supported by Xiamen University Malaysia (XMUM) under the XMUM Research Fund (XMUMRF) (Grant number: XMUMRF/2024-C14/ISFS/0002).

References

[1] Pulvirenti, G., Distefano, N., Leonardi, S. and Tollazzi, T. Are Double-Lane Roundabouts Safe Enough? A CHAID Analysis of Unsafe Driving Behaviors, *Safety*, 7(1) (2021), 20.

[2] Federal Highway Administration. Do you know the rules of the roundabout?, *FHWA brochure (FHWA-SA-17-055), U.S. Department of Transportation* (2017).

[3] Missouri Department of Transportation. Two-Lane Roundabouts: The Ins and Outs of Two-Lane Roundabouts, *Jefferson City, MO: Missouri Department of Transportation.*

[4] Tollazzi, T. Recent Alternative Types of Roundabouts. In: Alternative Types of Roundabouts: An Informational Guide, *Cham: Springer International Publishing* (2015), 117–155.

[5] Šarić, A. and Lovrić, I. Multi-lane Roundabout Capacity Evaluation, *Frontiers in Built Environment*, 3 (2017), 42.

[6] Hu, W. and Cicchino, J. B. Long-term crash trends at single- and double-lane roundabouts in Washington State, *Journal of Safety Research*, 70 (2019), 207–212.

[7] Robinson, B. W. and Rodegerdts, L. A. Capacity and performance of roundabouts: A summary of recommendations in the FHWA roundabout guide, *Proc. 4th Int. Symp. on Highway Capacity 2000. Transportation Research Circular E-C018* (2000), 422–433.

[8] Akçelik, R. Capacity and Performance Analysis of Roundabout Metering Signals, *Paper presented at TRB National Roundabout Conference, Vail, Colorado, USA* (22–25 May 2005).

[9] Wang, R. and Ruskin, H. J. Modelling Traffic Flow at Multi-Lane Urban Roundabouts, *International Journal of Modern Physics C*, 17(5) (2006), 693–710.

[10] Bared, J. G. and Afshar, A. M. Using Simulation to Plan Capacity Models by Lane for Two- and Three-Lane Roundabouts, *Transportation Research Record: Journal of the Transportation Research Board*, 2096(1) (2009), 8–15.

[11] Delle Monache, M. L., Hammond, S. and Piccoli, B. Riemann solver for a macroscopic double-lane roundabout model, *IFAC-PapersOnLine*, 51(9) (2018), 55–60.

[12] Cheah, Y. H. and Yeak, S. H. Modeling of Traffic Flow on Roundabouts, *Malaysian Journal of Fundamental and Applied Sciences*, 18 (2022), 343–366.

[13] Cheah, Y. H. and Yeak, S. H. Modeling and Simulation on Roundabout with Waiting System, *Proceedings of the International Conference on Mathematical Sciences and Statistics (ICMSS 2022), Atlantis Press* (2022), 303–318.